Journal of Solid Mechanics Vol. 4, No. 1 (2012) pp. 59-74

Free Vibrations of Three-Parameter Functionally Graded Plates Resting on Pasternak Foundations

J.E. Jam[1,*], S. Kamarian[2], A. Pourasghar[3], J. Seidi[2]

[1]*Composite Materials and Technology Center, MUT, Tehran, Iran*
[2]*Department of Mechanical Engineering, Ilam Branch, Islamic Azad University, Ilam, Iran*
[3]*Young Researchers Club, Islamic Azad University, Tehran Markaz- Branch, Tehran, Iran*

Received 5 December 2011; accepted 6 February 2012

ABSTRACT

In this research work, first, based on the three-dimensional elasticity theory and by means of the Generalized Differential Quadrature Method (GDQM), free vibration characteristics of functionally graded (FG) rectangular plates resting on Pasternak foundation are focused. The two-constituent functionally graded plate consists of ceramic and metal grading through the thickness. A three-parameter power-law distribution is considered for the ceramic volume fraction. The benefit of using a three-parameter power-law distribution is to illustrate and present useful results arising from symmetric, asymmetric and classic profiles. A detailed parametric study is carried out to highlight the influences of different profiles of fiber volume fraction, three parameters of power-law distribution and two-parameter elastic foundation modulus on the vibration characteristics of the FG plates. The main goal of the structural optimization is to minimize the weight of structures while satisfying all design requirements imposed. Thus, for the second aim of this paper, volume fraction optimization of FG plates with objective of minimizing the density to achieve a specified fundamental frequency is presented. The primary optimization variables are the three parameters of the volume fraction of ceramic. Since the optimization processes is complicated and too much time consuming, a novel meta–heuristic called Imperialist Competitive Algorithm (ICA) which is a socio-politically motivated global search strategy and Artificial Neural Networks (ANNs) are applied to obtain the best material profile through the thickness. The performance of ICA is evaluated in comparison with other nature inspired technique Genetic Algorithm (GA). Comparison shows the success of combination of ANN and ICA for design of material profile of FG plates. Finally the optimized material profile for the considered optimization problem is presented.

Keywords: Functionally graded plates; Pasternak foundation; Three-parameter power-law distribution; Optimization; Imperialist competitive algorithm; Artificial neural networks

1 INTRODUCTION

A NEW class of materials known as ‘‘functionally graded materials’’ (FGMs) has attracted much attention as advanced structural materials in many structural members used in situations where large temperature gradients are encountered. FGMs are achieved by gradually changing the composition of the constituent materials along one (or more) direction(s), usually in the thickness direction, to obtain smooth variation of material properties and optimum response to externally applied loading. FG structures are used in a variety of engineering applications

* Corresponding author. Tel.: +98 21 22935300, Fax: +98 21 22936578.
E-mail address: jejam@mail.com (J.E. Jam).

including aircraft, construction and transportation where strong, stiff and light structures are required. The advantages of these structures are that it provides high specific stiffness and strength for a low-weight consideration.

A lot of number of plates resting on elastic foundations with different shapes, size, and thickness variations and boundary conditions has been the subject of numerous investigations and those play an important role in aerospace, marine, civil, mechanical, electronic and nuclear engineering problems. For example these types of plate are used in various kinds of industrial applications such as the analysis of reinforced concrete pavement of the roads, airport runways and foundation of buildings. The static analysis, buckling and free vibration of FGM plates have been extensively investigated [1-3]. Malekzadeh [4] studied free vibration analysis of thick FG plates supported on two-parameter elastic foundations by using DQ method and based on the three-dimensional elasticity theory. Elasticity solution for free vibrations analysis of functionally graded fiber reinforced plates on elastic foundation was studied by Yas and Sobhani [5] , the results were indicated the advantages of using continuous grading fiber reinforced plate with graded fiber volume fraction over traditional discretely laminated plates.

Various material profiles through the functionally graded plate thickness can be illustrated by using a three-parameter power-law distribution. Recently, Tornabene [6] has used three-parameter power law distribution to study the dynamic behavior of functionally graded parabolic panels of revolution. Yas et al. [7] studied free vibration analysis and optimization of three-parameter functionally graded Euler–Bernoulli beams resting on two-parameter elastic foundations. One of the advantages of using three-parameter power-law distribution is the ability of controlling the materials volume fraction of FG structures for considered applications.

The fiber-reinforced composite material studied in the present work consists of alumina (ceramic) fibers embedded in aluminum (metal) matrix with the fiber volume fraction graded according to a three-parameter power-law distribution through thickness. The frequency parameter of plate is obtained by using numerical technique termed the Generalized Differential Quadrature Method (GDQM) based on the DQ technique [8]. The GDQ approach was developed by Shu and Coworkers [9, 10]. It approximates the spatial derivative of a function of given grid point as a weighted linear sum of all the functional value at all grid point in the whole domain. The computation of weighting coefficient by GDQ is based on an analysis of a high order polynomial approximation and the analysis of a linear vector space. The weighting coefficients of the first-order derivative are calculated by a simple algebraic formulation, and the weighting coefficient of the second-and higher-order derivatives are given by a recurrence relationship. The details of the GDQ method can be found in [9, 10]. For the first goal of this study, investigations are carried out to study the effects of wave numbers (m, n), various geometrical parameters (a/b, h/b), elastic foundation coefficients (Kw, Kg) and ceramic volume fraction on the frequencies.

As a second goal of this study, weight minimization of three-parameter FG plate with constraint on the natural frequency is presented. Optimization is implemented for various objective functions in mechanical problems, such as buckling loads [11], weight [12], stiffness [13], fundamental frequencies [11], deflection [12], etc. When the search space becomes large, enumeration is soon no longer feasible simply because it would take far too much time. In this it's needed to use a specific technique to find the optimal solution. In the present work, Imperialist Competitive Algorithm (ICA) is implemented that has recently been introduced by Atashpaz-Gargary and Lucas (2007) for dealing with different applications, such as designing PID controller [14], characterizing materials properties [15], error rate beam forming [16], designing vehicle fuzzy controller [17], etc. Imperialist Competitive Algorithm is a novel global search heuristic for optimization that uses imperialism an imperialistic competition process as a source of inspiration.

M. Abouhamze et al. [11] optimized stacking sequence of laminated cylindrical panels with respect to the first natural frequency and critical buckling load. They used Genetic Algorithm (GA) and Artificial Neural Networks (ANNs) for optimization. Artificial Neural Network (ANN) modeling is an equation-free, data-driven modeling technique that tries to emulate the learning process in the human brain by using many examples. ANN can be defined as a massive parallel-distributed information processing system that has a natural propensity for recognizing and modeling complicated input-output systems. The concept of neural networks has been introduced to different branches of engineering, analytical procedure of structural design, structural optimization problems and functionally graded materials [11, 18-20]. As a simple modeling technique, in this work, ANNs are employed to reproduce the behavior of FG plate both in fundamental frequency parameter and density in order to reduce the time of the optimization process. The considered ANNs are trained by training data sets obtained from GDQ method.

2 FGM PROPERTIES

Consider a thick FG plate rested on two-parameter elastic foundations as shown in Fig. 1. A Cartesian coordinate system (*x, y, z*) is used to label the material point of the plate in the unstressed reference configuration. The Young's modulus $E(z)$, Poisson's ratio $\nu(z)$ and mass density $\rho(z)$ of the FG plate can be expressed as a linear combination:

$$\begin{aligned} E(z) &= E_c V_c + E_m V_m \\ \rho(z) &= \rho_c V_c + \rho_m V_m \\ \nu(z) &= \nu_c V_c + \nu_m V_m \end{aligned} \tag{1}$$

where $\rho_m, E_m, \upsilon_m, V_m$ and $\rho_c, E_c, \upsilon_c, V_c$ represent mass density, Young's modulus, Poisson's ratio and volume fraction of the metal and ceramic constituent materials, respectively. In the present work, V_c is considered as follow [6]:

$$V_c(z) = [\frac{z}{h} + b(1 - \frac{z}{h})^c]^p \tag{2}$$

where volume fraction index p $(0 \le p \le \infty)$ and the parameters *b, c* dictate the material variation profile through the FG beam thickness. It should be noticed that the values of parameters *b* and *c* must be chosen so that $0 \le V_c \le 1$. The through-thickness variations of the fiber volume fraction for some profiles are illustrated in Fig. 2.

In Fig. 2 (a) the classical fiber volume fraction profiles are presented as special cases of the general distribution laws (2) by setting *b=0*. In Figs. 2 (b-c) by setting *b=1, c=2* and *b=1, c=4* symmetric and asymmetric profiles respect to the middle of plate $(\eta = 0\ ,\ \eta = \frac{z - h/2}{h})$ are obtained respectively. Some fiber volume fraction profiles are shown in Fig. 2 (d) for *b=0.2, c=2*.

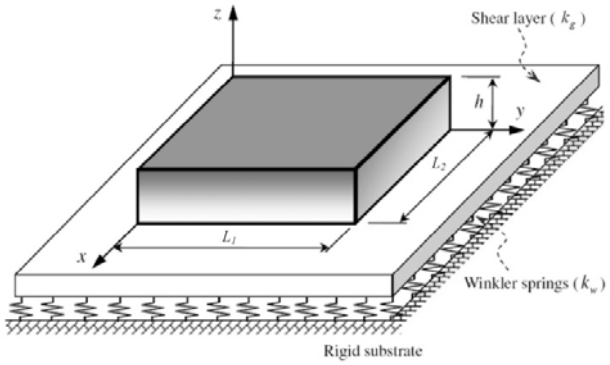

Fig.1
Geometry of the FG rectangular plate resting on elastic foundation.

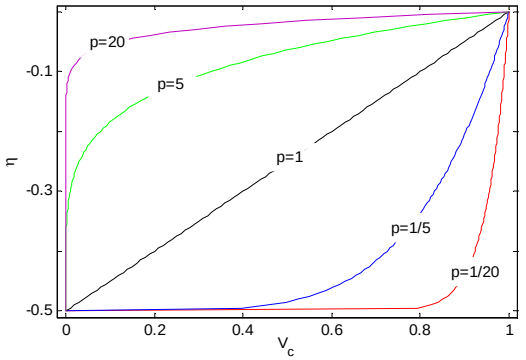

(a)

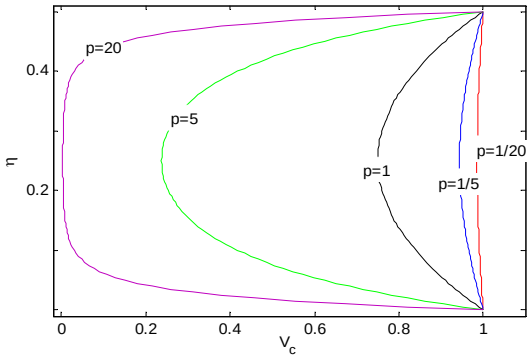

(b)

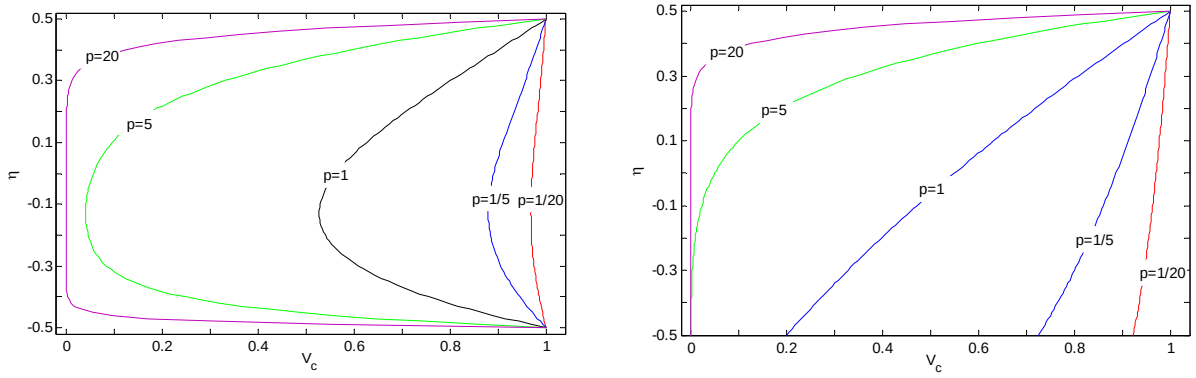

Fig.2
Variation of the ceramic volume fraction through the thickness in the FG plate a : $b=0$, b : $b=1$, $c=2$, c: $b=1$, $c=4$ d : $b=0.2$, $c=2$

3 ELASTICITY SOLUTION

The constitutive relations for the k th layer of the FG plate can be written as follows [5]:

$$\begin{Bmatrix}\sigma_x\\ \sigma_y\\ \varepsilon_z\\ \tau_{zy}\\ \tau_{xz}\\ \tau_{xy}\end{Bmatrix}=\begin{bmatrix}C_{11} & C_{12} & C_{13} & 0 & 0 & 0\\ C_{12} & C_{22} & C_{23} & 0 & 0 & 0\\ C_{13} & C_{23} & C_{33} & 0 & 0 & 0\\ 0 & 0 & 0 & C_{44} & 0 & 0\\ 0 & 0 & 0 & 0 & C_{55} & 0\\ 0 & 0 & 0 & 0 & 0 & C_{66}\end{bmatrix}\begin{Bmatrix}\varepsilon_x\\ \varepsilon_y\\ \varepsilon_z\\ \gamma_{zy}\\ \gamma_{xz}\\ \gamma_{xy}\end{Bmatrix} \tag{3}$$

In the absence of body forces, the governing equations are as follows [5]:

$$\begin{aligned}&\frac{\partial\sigma_x}{\partial x}+\frac{\partial\tau_{xy}}{\partial y}+\frac{\partial\tau_{xz}}{\partial z}=\rho\frac{\partial^2 u}{\partial t^2}\\ &\frac{\partial\tau_{xy}}{\partial x}+\frac{\partial\sigma_y}{\partial y}+\frac{\partial\tau_{yz}}{\partial z}=\rho\frac{\partial^2 v}{\partial t^2}\\ &\frac{\partial\tau_{xz}}{\partial x}+\frac{\partial\tau_{yz}}{\partial y}+\frac{\partial\sigma_z}{\partial z}=\rho\frac{\partial^2 w}{\partial t^2}\end{aligned} \tag{4}$$

Strain-displacement relations are expressed as [5]:

$$\begin{aligned}&\varepsilon_z=\frac{\partial w}{\partial z}\qquad \varepsilon_y=\frac{\partial v}{\partial y}\qquad \varepsilon_x=\frac{\partial u}{\partial x}\qquad \gamma_{xy}=\frac{\partial v}{\partial x}+\frac{\partial u}{\partial y}\\ &\gamma_{xz}=\frac{\partial w}{\partial x}+\frac{\partial u}{\partial z}\qquad \gamma_{yz}=\frac{\partial v}{\partial z}+\frac{\partial w}{\partial y}\end{aligned} \tag{5}$$

where u,v,w are displacement components along the x, y and z axes respectively. Upon substitution Eq. (5) into (3) and then into (4), the following equations of motion as matrix form are obtained in term of displacement components [5]:

$$\begin{bmatrix} L_{1x} & L_{1y} & L_{1z} \\ L_{2x} & L_{2y} & L_{2z} \\ L_{3x} & L_{3y} & L_{3z} \end{bmatrix} \begin{Bmatrix} u \\ v \\ w \end{Bmatrix} = \begin{Bmatrix} \rho\ddot{u} \\ \rho\ddot{v} \\ \rho\ddot{w} \end{Bmatrix} \tag{6}$$

For a simply supported rectangular plate, the boundary conditions can be expressed on the *x*-constant and on the *y*-constant edges as:

$$u_{,x} = v = w = 0 \quad , \quad u = v_{,y} = w = 0 \tag{7}$$

Moreover the lower and upper surfaces of the plate are traction free:

$$\begin{aligned} &\tau_{zx} = \tau_{zy} = 0 \quad and \quad \sigma_z = k_w w - k_g \Delta w \quad at \quad z = 0 \\ &\sigma_z = \tau_{zx} = \tau_{zy} = 0 \quad at \quad z = h \end{aligned} \tag{8}$$

Using the method of separation of variables, it is possible to seek solutions that are harmonic in time and whose frequency is ω. The displacements can be written as follows:

$$\begin{aligned} u &= \sum_{m=1}^{\infty}\sum_{n=1}^{\infty} U(z)\cos(\beta_m x)\sin(p_n y)e^{i\omega t} \\ v &= \sum_{m=1}^{\infty}\sum_{n=1}^{\infty} V(z)\sin(\beta_m x)\cos(p_n y)e^{i\omega t} \\ w &= \sum_{m=1}^{\infty}\sum_{n=1}^{\infty} W(z)\sin(\beta_m x)\sin(p_n y)e^{i\omega t} \end{aligned} \tag{9}$$

where $\beta_m = \dfrac{m\pi}{a}\ (m = 1,2,...)$ and $p_n = \dfrac{n\pi}{b}\ (n = 1,2,...)$, m and n are wave numbers along x and y directions respectively. Inserting these displacement components into the equations of motion (6), one obtains a set of coupled and variable coefficients differential equations.

$$\begin{aligned} &-C_{11}\beta_m{}^2 U - C_{12}\beta_m p_n V + C_{13}\beta_m \frac{\partial W}{\partial z} - p_n{}^2 C_{66} U - C_{66}\beta_m p_n V + \frac{\partial C_{55}}{\partial z}\beta_m W + C_{55}\beta_m \frac{\partial W}{\partial z} \\ &+ \frac{\partial C_{55}}{\partial z}\frac{\partial U}{\partial z} + C_{55}\frac{\partial^2 U}{\partial z^2} = -\rho\omega^2 U \\ &-C_{66}\beta_m p_n U - C_{66}\beta_m{}^2 V - C_{12}\beta_m p_n U - C_{22}p_n{}^2 V + C_{23}p_n \frac{\partial^2 W}{\partial z} + \frac{\partial C_{44}}{\partial z}\frac{\partial V}{\partial z} + C_{44}\frac{\partial^2 V}{\partial z^2} \\ &+ \frac{\partial C_{44}}{\partial z}p_n W + C_{44}p_n \frac{\partial W}{\partial z} = -\rho\omega^2 V \\ &-C_{55}\beta_m{}^2 W - C_{55}\beta_m \frac{\partial U}{\partial z} - C_{44}p_n \frac{\partial V}{\partial z} - C_{44}p_n{}^2 W - \frac{\partial C_{13}}{\partial z}\beta_m U - C_{13}\beta_m \frac{\partial U}{\partial z} - \frac{\partial C_{23}}{\partial z}p_n V \\ &-C_{23}p_n \frac{\partial V}{\partial z} + \frac{\partial C_{33}}{\partial z}\frac{\partial W}{\partial z} + C_{33}\frac{\partial^2 W}{\partial z^2} = -\rho\omega^2 W \end{aligned} \tag{10}$$

A semi – analytical procedure with the aid of DQ technique was recently developed [21]. In this method, the *n*th order of a continuous function $f(x,z)$ with respect to x at a given point x_i can be approximated as a linear sum of weighting values at all of the discrete point in the domain of x , i.e. [9, 10]

$$\frac{\partial f^{n(x_i,z)}}{\partial x^n} = \sum_{k=1}^{N} c_{ik}^n f(x_{ik},z) \quad , \quad i = 1,2,...,N \ , \ n = 1,2,N-1 \tag{11}$$

where N is the number of sampling points, and $c_{ij}^{\ n}$ is the x^i dependent weight coefficients.

4 NEURAL NETWORK MODELING

The basic element of an NN is the artificial neuron as shown in Fig. 3 which consists of three main components namely as weights, bias, and an activation function. Each neuron receives inputs x^1; x^2; . . . ; x^n, attached with a weight w^i which shows the connection strength for that input for each connection. Each input is then multiplied by the corresponding weight of the neuron connection. A bias b_i can be defined as a type of connection weight with a constant nonzero value added to the summation of inputs and corresponding weights u, given by

$$u_i = \sum_{j=1}^{H} w_{ij} x_j + b_i \tag{12}$$

The summation u_i is transformed using a scalar-to-scalar function called an ‘‘activation or transfer function’’, $F(u_i)$ yielding a value called the unit’s ‘‘activation’’, given by:

$$Y_i = f(u_i) \tag{13}$$

Activation functions serve to introduce nonlinearity into NNs which makes NNs so powerful. NNs are commonly classified by their network topology (i.e. feedback, feed forward) and learning or training algorithms (i.e. supervised, unsupervised). There is no well-defined rule or procedure to have optimal network architecture. In this work, the feed forward Multi-Layer Perceptron (MLP) network has been applied. MLP networks are one of the most popular and successful neural network architectures which are suited to a wide range of applications such as prediction and process modeling. The neural network architecture adopted in the present work has two hidden layers which has high accuracy and has been used for various applications. Fig.4 illustrates the topology of a simple, fully connected four-layer MLP network.

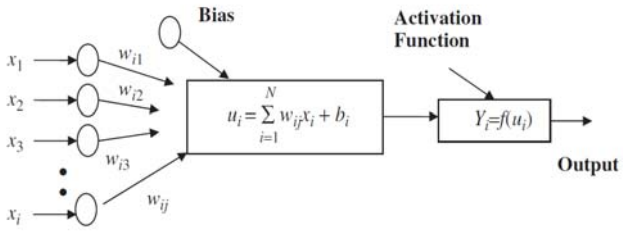

Fig.3
Basic elements of an artificial neuron.

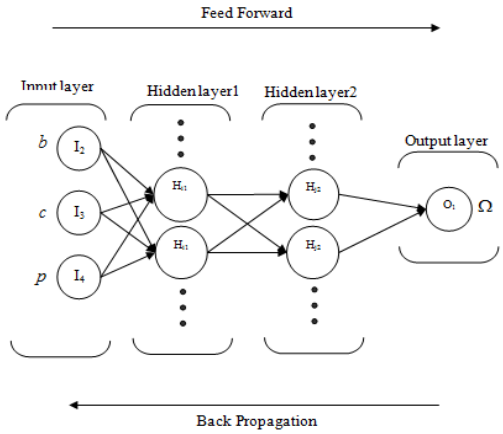

Fig.4
Schematic diagram of ANN model.

5 IMPERIALIST COMPETITIVE ALGORITHM

Like other evolutionary algorithms, ICA starts with an initial population called countries that are divided in two types: imperialists (in optimization terminology, countries with least cost) and colonies (the remained countries). In ICA, the more powerful imperialist, have the more colonies. Based on the power of countries (the counterpart of fitness value in Genetic Algorithm which is inversely proportional to its cost), all of them are divided among the mentioned imperialists. Starting the competition, imperialists attempt to achieve more colonies and colonies in each of them start to move toward their relevant imperialist which this movement is shown in Fig. 5. In this movement θ, x are random numbers with uniform distribution as illustrated in Eq. (14) [22] and d is the distance between colony and the imperialist. In Eq. (14), β and γ are parameters that modify the area that colonies randomly search around the imperialist. Weak empires will lose their power and will be eliminated from the competition (in another word, they will be collapsed) and the powerful ones will be improved and remain. At last, only one imperialist will remain that in this stage, colonies have the same position and power as the imperialist.

$$x \sim U(0\ ,\ \beta \times d)\quad ,\quad \theta \sim U(-\gamma, \gamma) \tag{14}$$

In imperialistic competition which is shown in Fig. 6, all empires try to take possession of colonies of other empires and control them. Based on the total power of empires which is observed in Eq. (15) [22], the more powerful an empire, the more likely it will possess the colonies. Imperialistic competition can be modeled as Fig. 6.

$$T.C._n = Cost\,(imperialist_n) + \zeta\ mean\{Cost(colonoes\ \ of\ \ impire_n)\} \tag{15}$$

The main steps in the ICA are summarized as follows:

- Select some random points on the function and initialize the empires.
- Move the colonies toward their relevant imperialist (Assimilating).
- If there is a colony in an empire which has lower cost than that of imperialist, exchange the - positions of that colony and the imperialist.
- Compute the total cost of all empires (related to the power of both imperialist and its colonies).
- Pick the weakest colony (colonies) from the weakest empire and give it (them) to the empire that has the most likelihood to possess it (imperialistic competition).
- Eliminate the powerless empires.
- If there is just one empire, stop, if not go to 2.

Also, the flowchart of the ICA is shown in Fig. 7. More details about the proposed algorithm are found in [22].

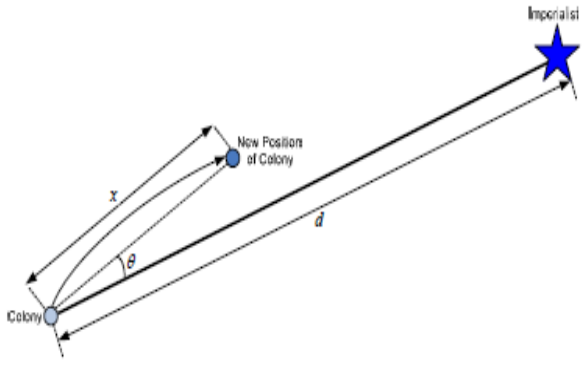

Fig.5
Motion of colonies toward their relevant imperialist.

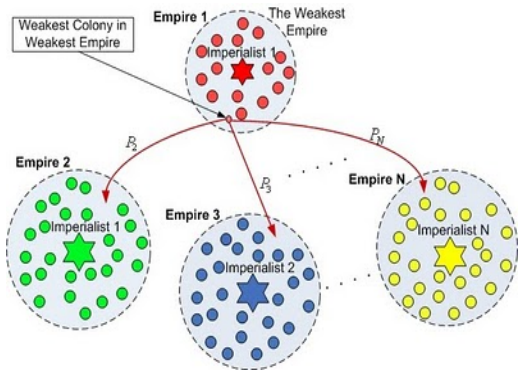

Fig.6
Imperialistic competition.

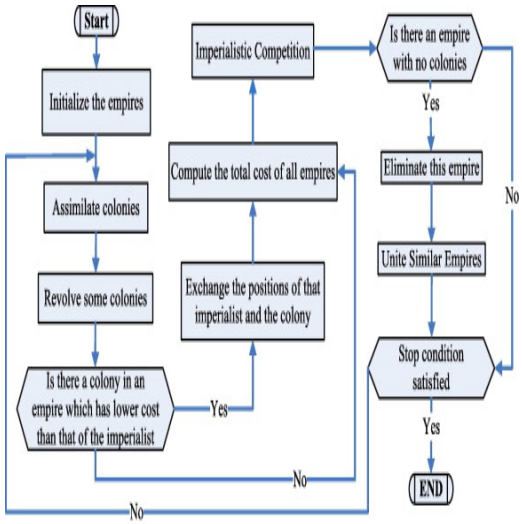

Fig.7
Flowchart of the Imperialistic competitive algorithm.

6 RESULTS AND DISCUSSION

6.1 Free vibration analysis

To validate the analysis, first, numerical results for a FGM rectangular plate without elastic foundation are compared with similar ones in the literature and listed in Table 1. The comparison shows that the present results agree well with those in the literatures. As noticed, fast rate of convergence of the GDQM is evident and it is founded that only 13 DQ grid in the thickness direction can yield accurate results. Further validation of the present results is shown for isotropic plate on elastic foundation in Table 2. These comparisons show that the results from the present method are in good agreement with the existing results, thus verifying the reliability and accuracy of the present method.

In this section, we characterize the response of FG rectangular plate rested on Pasternak foundation. In this study, ceramic and metal are particle mixed to form the functionally graded material. The relevant material properties for the constituent materials are shown in Table 3. [24]. The non-dimensional frequency parameter of FG plate and foundations stiffness used in the present work are defined by:

$$\Omega = \omega h\sqrt{\rho_c / E_c}\ ,\ Kg = kg\, L_1^2 / D_c\ ,\ Kw = kw\, L_1^4 / D_c\ ,\ D_c = E_c h^3 / 12(1-\nu_c^2)$$

Table 1
Convergence behavior and accuracy of the first four non-dimensional natural frequencies of a simply supported FG plate against the number of DQ grid points (h/b=0.5).

		Mode (n, m)			
P		(1,0)	(1,1)	(2,0)	(1,2)
0.5	N=7	0.483544	0.823838	1.335584	1.54482
	N=9	0.483166	0.823	1.333849	1.542636
	N=13	0.482935	0.822527	1.332923	1.541478
	N=20	0.482849	0.822358	1.332605	1.541085
	[3]	0.4835	0.8233	1.3339	1.5425
4	N=7	0.358102	0.599857	0.959461	1.104807
	N=9	0.357663	0.59935	0.958488	1.103291
	N=13	0.357754	0.599487	0.958751	1.103656
	N=20	0.357758	0.599494	0.958764	1.103674
	[3]	0.3579	0.5997	0.9591	1.104

Table 2
Comparison of the first three non-dimensional natural frequencies of an isotropic plate on the elastic foundation (N=13, K_g=10) .

$h / L_1 = 0.5$		$h / L_1 = 0.2$					
	K_w	Ω_{11}	Ω_{12}	Ω_{13}	Ω_{11}	Ω_{12}	Ω_{13}
Present	10	1.657742	2.687861	3.827391	2.253924	4.415035	7.248745
[4]		1.6577	2.6879	3.8274	2.2539	4.415	7.2488
[23]		1.6577	2.6879	3.8274	2.2539	4.415	7.2488
Present	100	1.743700	2.70962	3.832129	2.429988	4.498601	7.29475
[4]		1.7437	2.7096	3.8321	2.43	4.4986	7.2948
[23]		1.7437	2.7096	3.8321	2.43	4.4986	7.2948

Table 3
Material properties [24]:

Material properties	
E_c (Gpa)	380
E_m (Gpa)	70
ρ_c (kg / m^3)	3800
ρ_m (kg / m^3)	2707

The influence of the parameters *b, c, p* on the fundamental frequency parameter and density of a FG plate is shown in Figs. 8-9. The new and interesting result is that by using the three-parameter volume fraction, we can control the profile of ceramic volume fraction. In other words, there are different values of density for a constant frequency and on the other hand, for a constant density, we can have different values for frequency parameter. The first normalized frequencies of different types of FG plates are compared with each other in Table 4. for different values of h/L_1 ratio and volume fraction index *p*. In this table, the volume fraction profiles through thickness are classical for *b=0*, symmetric for *b=1*, *c=2* and asymmetric for *b=1*, *c=4*. It can be concluded from Table 4. that the normalized frequencies of symmetric profile are larger than that of other types of FG plates for different values of *p* and h/L_1 ratio. Also, it can be found that for various values of h/L_1 ratio, normalized frequencies of classic profile are smaller than that of other types of FG plates.

Table 4
Comparison of fundamental normalized frequencies of different types of FG plates for different values of h/L_1 ratio ($L_1/L_2=1$, $Kw=100$, $Kg=10$, $n=1$, $m=1$).

h/L_1	Type of FG	p						
		0	1	2	5	10	50	∞
0.2	*Classic*	0.2903	0.2636	0.2562	0.2542	0.2552	0.2541	0.2519
	Symmetric	0.2903	0.2897	0.2887	0.2844	0.2773	0.2607	0.2519
	Asymmetric	0.2903	0.2879	0.2843	0.2743	0.2667	0.2566	0.2519
0.4	*Classic*	0.9545	0.7785	0.7070	0.6610	0.6371	0.5806	0.5605
	Symmetric	0.9545	0.9438	0.9310	0.8830	0.7601	0.6029	0.5605
	Asymmetric	0.9545	0.9211	0.8800	0.7679	0.6757	0.5881	0.5605
0.5	*Classic*	1.3020	0.9976	0.8855	0.8075	0.7876	0.7248	0.7006
	Symmetric	1.3020	1.2737	1.2417	1.1024	0.9472	0.7527	0.7006
	Asymmetric	1.3020	1.2225	1.1358	0.9493	0.8397	0.7344	0.7006

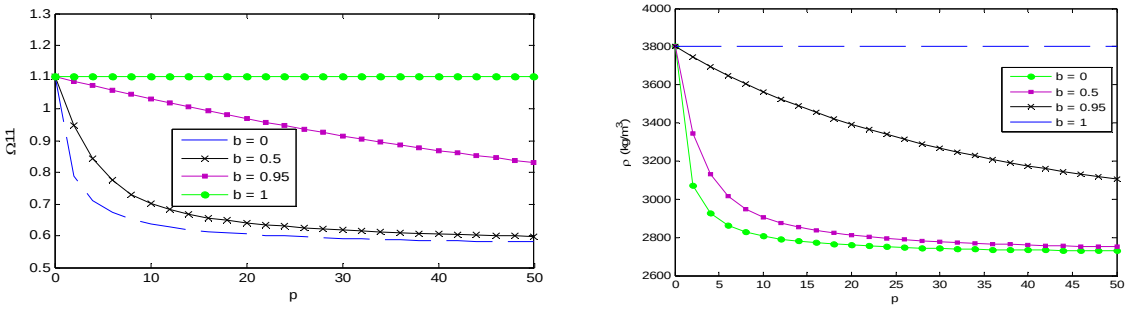

(a) (b)

Fig.8
Variation of the first non-dimensional natural frequency and density of FG plate vs. the power-law exponent p for various values of the parameter b ($-1\le b\le 0$, $c=1$, $h/L_1=0.4$, $Kw=1000$, $Kg=10$)

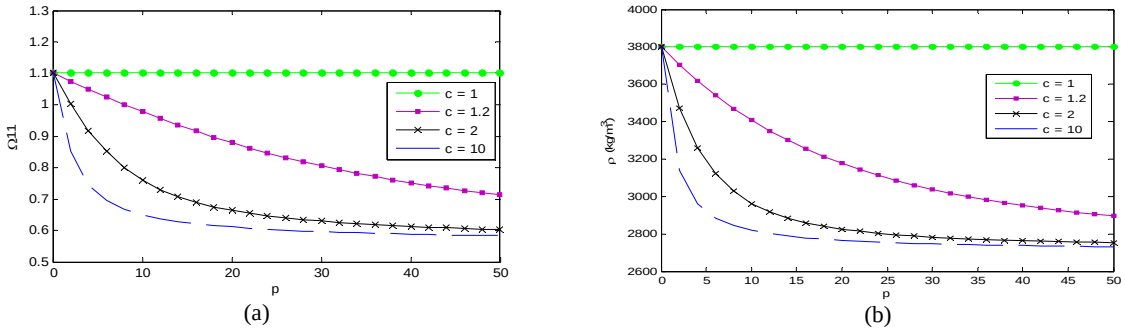

(a) (b)

Fig.9
Variation of the first non-dimensional natural frequency and density of FG plate vs. the power-law exponent p for various values of the parameter c ($b=1, 1\le c\le 4$, $c=1$, $h/L_1=0.4$, $Kw=1000$, $Kg=10$)

The numerical results are tabulated in Table 5. for symmetric FG plates and different values of foundation stiffness parameters. The effects of the elastic foundation coefficients on the first three non-dimensional natural frequencies for different values of *h*/L1 ratio of a square FG plate are also shown in Table 6. It is observed from these tables that both Winkler and shearing layer elastic coefficients have significant effects on the non-dimensional frequencies of FG plate. Results show that as the shearing layer elastic coefficient increases the effect of Winkler

coefficients on natural frequency parameter decreases and so on with increasing Winkler coefficients, the effect of shearing layer elastic coefficient on natural frequency decreases.

Table 5
Variation of the normalized natural frequencies of symmetric FG plate on elastic foundation ($L_1/L_2=1,\ b=1,\ c=2,\ n=1,\ m=1$)

h/L_1	$K_w,\ K_g$	p						
		0	1	2	5	10	50	∞
0.2	10, 1	0.2213	0.2165	0.2115	0.1972	0.1793	0.1471	0.1311
	100, 10	0.2903	0.2897	0.2887	0.2844	0.2773	0.2607	0.2519
	1000, 100	0.5511	0.5250	0.5010	0.4422	0.3817	0.3019	0.2802
0.4	10, 1	0.7153	0.6938	0.6727	0.6158	0.5537	0.4733	0.4342
	100, 10	0.9545	0.9438	0.9310	0.8830	0.7601	0.6029	0.5605
	1000, 100	1.1021	1.0499	1.0017	0.8830	0.7601	0.6029	0.5605
0.5	10, 1	1.0055	0.9729	0.9413	0.8575	0.7675	0.6585	0.6076
	100, 10	1.3020	1.2737	1.2417	1.1024	0.9472	0.7527	0.7006
	1000, 100	1.3777	1.3123	1.2518	1.1024	0.9472	0.7527	0.7006

Table 6
The first three non-dimensional natural frequency of a FG plate on the elastic foundation ($L_1/L_2=1, b=1,\ c=2$)

h/L_1	K_w	$K_g=0$			$K_g=10$			$K_g=100$		
		Ω_{11}	Ω_{22}	Ω_{33}	Ω_{11}	Ω_{22}	Ω_{33}	Ω_{11}	Ω_{22}	Ω_{33}
0.2	0	0.1846	0.5571	0.9684	0.2558	0.6491	1.0777	0.4422	0.8830	1.3120
	10	0.1889	0.5584	0.9692	0.2588	0.6501	1.0782	0.4422	0.8830	1.3120
	10^2	0.2238	0.5704	0.9761	0.2844	0.6590	1.0824	0.4422	0.8830	1.3124
	10^3	0.4262	0.6695	1.0362	0.4422	0.7347	1.1204	0.4422	0.8830	1.3158
0.4	0	0.5571	1.3856	2.2244	0.8830	1.6719	2.3756	0.8830	1.6719	2.3756
	10	0.5781	1.3943	2.2302	0.8830	1.6719	2.3756	0.8830	1.6719	2.3756
	10^2	0.7204	1.4577	2.2706	0.8830	1.6720	2.3757	0.8830	1.6720	2.3757
	10^3	0.8830	1.6218	2.3538	0.8830	1.6728	2.3757	0.8830	1.6728	2.3757
0.5	0	0.7612	1.8041	2.8607	1.0869	1.9927	2.9603	1.1024	2.0106	2.9631
	10	0.7974	1.8203	2.8717	1.0932	1.9930	2.9603	1.1024	2.0106	2.9631
	10^2	0.9940	1.9076	2.9219	1.1024	1.9949	2.9605	1.1024	2.0106	2.9631
	10^3	1.1024	1.9968	2.9580	1.1024	2.0036	2.9614	1.1024	2.0108	2.9631

Fig. 10 shows the effect of Winkler elastic coefficient on the first non-dimensional natural frequency of plate for different values of shearing layer elastic coefficients. The most effective range of Winkler foundation stiffness in increasing the non-dimensional natural frequency is from 1 to 1000. It is also observed for the large values of Winkler elastic coefficient, the shearing layer elastic coefficient has less effect and the results become independent of it. In other words, the non-dimensional natural frequencies converge with increasing Winkler foundation stiffness. The influence of shearing layer elastic coefficient on the first non-dimensional natural frequency is shown in Fig. 11. The most effective range of shearing layer foundation stiffness in increasing the non-dimensional natural frequency is from 1 to 100. It results the variations of Winkler elastic coefficient has no effect on the non-dimensional natural frequency for Kg $\geq$ 100.

The effect of length to width ratio of the FG plate on the first non-dimensional natural frequency is shown in Fig. 12. It results that the non-dimensional natural frequency decreases with increasing the L_1/L_2 ratio and then remain almost unaltered for L_1/L_2 greater than 5 at different values of Winkler and shearing layer elastic coefficients.

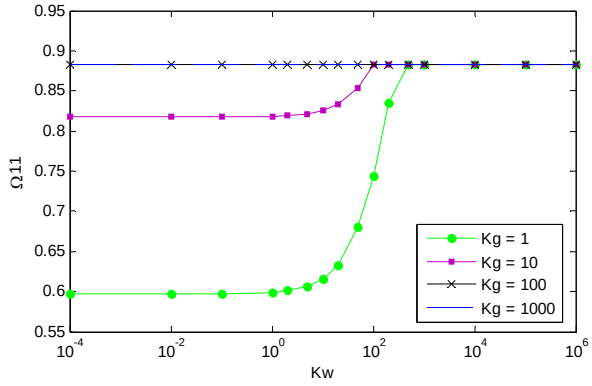

Fig.10
Variation of the first non-dimensional natural frequency of FG plate resting on elastic foundation vs. Winkler elastic coefficient for different shearing layer elastic coefficients ($b=1, c=2, p=5, h/L_1=0.4$)

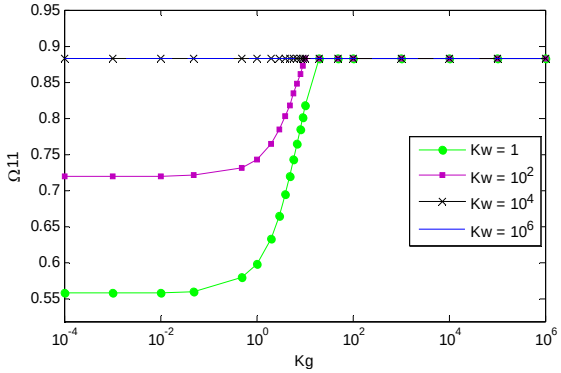

Fig.11
Variation of the first non-dimensional natural frequency of FG plate resting on elastic foundation vs. shearing layer elastic coefficients for different Winkler elastic coefficient ($b=1, c=2, p=5, h/L_1=0.4$)

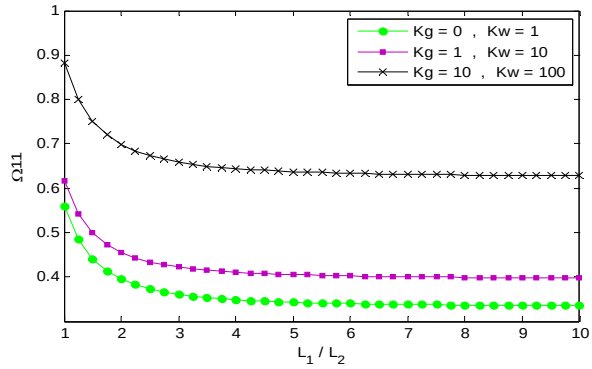

Fig.12
The effect of length to width ratio of the CGFR plate (L1/L2) on the non-dimensional natural frequency ($b=1, c=2, p=5, h/L_1=0.4$)

6.2 Optimization procedure

The objective of optimization in this paper is to find the best values of the parameters *b, c, p* in the three-parameter power law distribution for minimizing the density of FG plate to achieve a specified fundamental frequency parameter. The h/L_1 ratio is considered to be 0.4. There is an important point that considered parameters must be obtained so that the ceramic volume fraction is between zero and one ($0 \le V_c \le 1$). The parameters are considered in the following ranges: $0 \le b \le 1, 1 \le c \le 20, \ 0 \le p \le 40$

Therefore, the constrained optimization problem is defined as:

$$\begin{aligned} &\textit{Minimize} && f(b,c,p)=\rho \\ &\textit{Subject to} && \begin{cases} \Omega \geq 0.75 \\ 0 \leq V_c \leq 1 \\ 0 \leq b \leq 1\,,\ 0 \leq c \leq 20\,,\ \ 0 \leq p \leq 40 \end{cases} \end{aligned}$$

If GDQ method is applied for frequency parameters, the optimization process becomes so complicated and time consuming. For example even if the increment of the parameters (*b, c, p*) is assumed 0.05, the formed discrete space contains more than 6,400,000 design choices to be searched for an optimum point. Also, if it is assumed that the process of one search takes 0.2 second in average, the optimization process takes more than 350 hours. Thus in the present work, two ANNs (NN_dens for prediction of density and NN_vibr for prediction of frequency of FG plate) and ICA are implemented for increasing the speed of optimization. The MLP networks have been used having two hidden layers. A program was developed in MATLAB which handles the trial and error process automatically. The program tries varying number of hidden layers neurons is tested from two up to twenty for a 500 epochs for 5 times for different back propagation training algorithms and activation that the results are tabulated in Table 7. The ability of trained networks to reproduce the fundamental frequency parameter and density of plate is shown in Fig. 13 for 36 test points which selected far from the training point randomly. In this figure comparison is made between the ANN results for natural frequency and density with similar ones obtained from numerical method, namely GDQM. As noticed the results are so close for all 36 test points. The accuracy of the trained ANNs is also shown in Tables 8 and 9 for several test points. Since the neural networks have been accurately designed, they can be implemented in ICA by simulating fundamental frequency parameter and density.

Table 7
Architecture of the trained neural networks for free vibration and density .

Name	First layer		Second layer		Output layer	
	Neuron	function	Neuron	function	Neuron	function
Net_dens	11	Tangent sigmoid	8	Tangent sigmoid	1	linear
Net_vibr	10	Tangent sigmoid	9	Tangent sigmoid	1	linear

Table 8
Comparison of various predicted values of density of FG plate versus numerical data .

Number of test	Value of parameters			$\rho(kg/m^3)$		Related Error
	b	*c*	*p*	GDQ	NN_dens	
1	0.51	4.2	5.8	2783.0	2783.2	0.007%
2	0.12	2.2	1.3	3216.7	3217.4	0.022%
3	0.77	9.0	15.8	2772.2	2772.1	0.004%
4	0.95	5.5	14	2788.7	2788.7	0.000%
5	0.25	7.0	4.5	2906.5	2906.3	0.007%

Table 9
Comparison of various predicted values of fundamental frequency parameter of FG plate versus numerical data

Number of test	Value of parameters			Ω_{11}		Related Error
	b	*c*	*p*	GDQ	NN_vibr	
1	6.25	6.60	7.00	0.6567	0.6565	0.031%
2	0.85	4.00	14.20	0.6221	0.6222	0.016%
3	0.66	5.28	8.93	0.6453	0.6453	0.000%
4	0.90	8.00	14.39	0.6208	0.6210	0.032%
5	0.72	3.90	10.40	0.6373	0.6374	0.016%

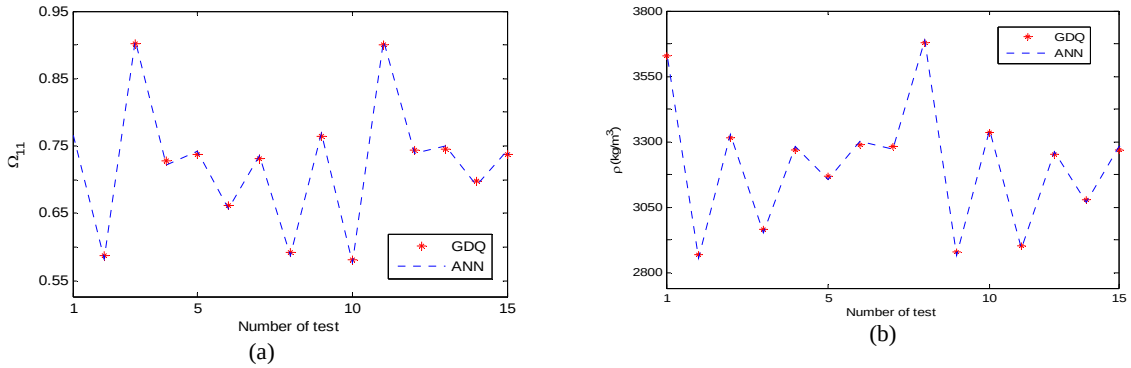

Fig.13
Comparison of various predicted values of density and fundamental frequency parameter versus numerical data.

Here, optimization is investigated for the FG plate. Table 10. shows the parameters of ICA used to find the optimal solution. As shown in this figure ICA has reached to the optimal values of [b=0.82, c=1.7, p=7.2] which leads the 2976.0 for value of the objective function. The performance of ICA is compared with other nature inspired technique Genetic Algorithm (GA). Comparison shows that ICA performs better than GA. This fact is shown in Table 11. It should be mentioned that the process of optimization in ICA took less than 2 minutes. It means CPU time is reduced by a considerable amount. Fig. 14 shows the optimized material profile for the considered optimization problem obtained by combination of ICA and ANN.

Table 10
Parameters of ICA approach

Parameters	Value
Number of initial countries	70
Number of initial imperialists	5
Number of decades	80
Revolution rate	0.4
β	2
γ	0.5
ζ	0.06

Table 11
Comparison between the Imperialist competitive Algorithm and genetic algorithm

Algorithm	Optimum parameters			$\rho(kg/m^3)$
	b	c	p	
ICA	0.82	1.70	7.20	2976.3
GA	0.69	2.98	4.05	2988.9

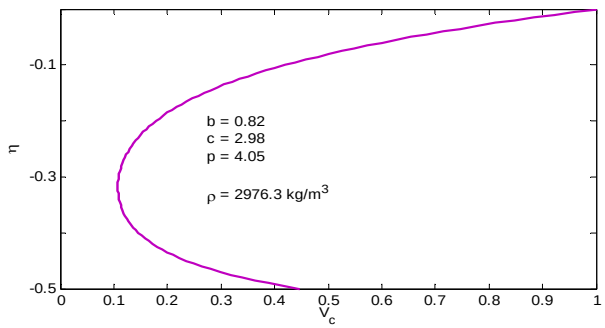

Fig.14
Optimized material profile for the FG plate obtained by ICA .

7 CONCLUSIONS

In this paper, free vibration of three-parameter FG rectangular plate rested on Pasternak was studied. Free vibration of FG plate was analyzed based on the three-dimensional elasticity theory and by means of GDQ method. The effect of the power-law exponent, power-law distribution choice and elastic foundation modulus on the natural frequencies of FG plates was investigated in this research work. In the next step, volume fraction optimization of three-parameter FG rectangular plate with respect to the density with constraint on the frequency parameter was studied. Imperialist Competitive Algorithm and Artificial Neural Networks were performed to obtain the best material profile through the thickness to find the optimal solution. From this study, some conclusions can be made:

- It has been found that the convergence of the GDQ results is very fast. The numerical results obtained by using only seven grid points agree very well with those in the literature.
- Results show that normalized frequencies of symmetric and classic profiles are larger and smaller than that of other types of FG plates respectively for different values of p and h/L_1 ratio.
- The most effective ranges of shearing layer elastic coefficient and Winkler foundation stiffness in increasing the non-dimensional natural frequencies is from 1 to 100 and 1 to 1000 respectively.
- It is observed that for the large values of Winkler elastic coefficient, the shearing layer elastic coefficient has less effect on the normalized frequency and the results become independent of it.
- It results the non-dimensional natural frequency decreases with increasing the L_1/L_2 ratio and then remain almost unaltered for L_1/L_2 greater than 5 at different values of Winkler and shearing layer elastic coefficients.
- By using three-parameter power law distribution, it is possible to control the materials volume fraction of FG structures for considered applications.
- ICA can be applied for engineering optimization problems especially for those related to the FG structures.
- Combination of NN and ICA reduces the CPU time by a considerable amount with losing negligible accuracy.
- The performance of ICA is better than other nature inspired technique Genetic Algorithm. In other word, the results obtained by ICA are more optimized than GA.

REFERENCES

[1] Hosseini-Hashemi Sh., Akhavan H., Rokni Damavandi Taher H., Daemi N., Alibeigloo A., 2010, Differential quadrature analysis of functionally graded circularand annular sector plates on elastic foundation, *Materials and Design* **31**: 1871–1880.

[2] Naderi A., Saidi A.R., 2011, Exact solution for stability analysis of moderately thick functionally graded sector plates on elastic foundation, *Composite Structures* **93**: 629–638.

[3] Matsunaga H., 2008, Free vibration and stability of functionally graded plates according to a 2D higher-order deformation theory, *Composite Structures* **82**: 499–512.

[4] Malekzadeh P., 2009, Three-dimensional free vibration analysis of thick functionally graded plates on elastic foundations, *Composite Structures* **89**: 367–373.

[5] Yas M.H., Sobhani B., 2010, Free vibration analysis of continuous grading fibre reinforced plates on elastic foundation, *International Journal of Engineering Science* **48**: 1881-1895.

[6] Viola E., Tornabene F., 2010, Free vibrations of three-parameter functionally graded parabolic panels of revolution, *Mech Res Commun* **163**: 51-59.

[7] Yas M. H., Kamarian S., Eskandari J., Pourasghar A., 2012, Optimization of functionally graded beams resting on elastic foundations, *Journal of Solid Mechanic*.

[8] Bellman R., Kashef B.G., Casti J., 1972, Differential quadrature: a technique for a rapid solution of non linear partial differential equations, *Journal of Computational Physics* **10**: 40–52.

[9] Shu C., 2000, Differential quadrature and its application in engineering, Springer, Berlin.

[10] Shu C., Richards BE., 1992, Application of generalized differential quadrature to solve two-dimensional incompressible Navier Stockes equations, *International Journal Numer Meth Fluid* **15**: 791-798.

[11] Abouhamze M., Shakeri M., 2007, Multi-objective stacking sequence optimization of laminated cylindrical panels using a genetic algorithm and neural networks, *Composite Structures* **81**: 253–263.

[12] Walker M., Smith R., 2003, A technique for the multi objective optimization of laminated composite structures using genetic algorithms and finite element analysis, *Composite Structures* **62**: 123–128.

[13] Jacob L. Pelletier, Senthil S. Vel., 2006, Multi-objective optimization of fiber reinforced composite laminates for strength, stiffness and minimal mass, *Computers and Structures* **84**: 2065–2080.

[14] Atashpaz-Gargari E., Hashemzadeh F., Rajabioun R., Lucas C., 2008, Colonial competitive algorithm, a novel approach for PID controller design in MIMO distillation column process, *International Journal of Intelligent Computing and Cybernetics* **1**: 337–355.

[15] Biabangard-Oskouyi A., Atashpaz-Gargari E., Soltani N., Lucas C., 2009, Application of imperialist competitive algorithm for materials property characterization from sharp indentation test, *International Journal of Engineering Simulation* 11–12.

[16] Khabbazi A., Atashpaz E., Lucas C., 2009, Imperialist competitive algorithm for minimum bit error rate beam forming, *International Journal Bio-Inspired* **1**: 125 - 133.

[17] A. M. Jasour, E. Atashpaz, C. Lucas, 2008, Vehicle fuzzy controller design using imperialist competitive algorithm, Second Iranian Joint Congress on Fuzzy and Intelligent Systems, Tehran, Iran.

[18] Jodaei A., Jalal M., Yas M.H., 2012, Free vibration analysis of functionally graded annular plates by state-space based differential quadrature method and comparative modeling by ANN, *Composites: Part B* **43**: 340-353.

[19] Ootao Y., Tanigawa Y., Nakamura T., 1999, Optimization of material composition of FGM hollow circular cylinder under thermal loading, *a neural network approach Composites Part B* **30**: 415–422.

[20] Han X., Xu D., Liu G.R., 2003, A computational inverse technique for material characterization of a functionally graded cylinder using a progressive neural network, *Neuro computing* **51**: 341 – 360.

[21] W.Q. Chen, Z.G. Chen, 2003, Elasticity solution for free vibration of laminated beam, *Composite Structures* **62**: 75–82.

[22] Atashpaz-Gargari E., Lucas C., 2007, imperialist competitive algorithm: An algorithm for optimization inspired by imperialistic competition, IEEE congress on evolutionary computation 4661-4667.

[23] D. Zhou, YK. Cheung, SH. Lo, FTK. Au, 2004,Three-dimensional vibration analysis of rectangular thick plates on Pasternak foundation, *International Journal for Numerical Methods in Engineering* **59** : 1313–1334.

[24] Shakeri M., Akhlaghi M., Hoseini S.M., 2006, Vibration and radial wave propagation velocity in functionally graded thick hollow cylinder **76**: 174–181.